Available online at www.sciencedirect.com
ScienceDirect
Catalysis Today 130 (2008) 283–291
CATALYSIS TODAY
www.elsevier.com/locate/cattod

Effect of the preparation method on the structural stability and hydrodesulfurization activity of NiMo/SBA-15 catalysts

P. Rayo [a], Mohan S. Rana [a], J. Ramírez [a,b,*], J. Ancheyta [a], A. Aguilar-Elguézabal [c]

[a] *Instituto Mexicano del Petróleo, Eje Central Lázaro Cárdenas 152, México, DF 07730, Mexico*
[b] *UNICAT, Departamento de Ingeniería Química, Facultad de Química, UNAM, Cd. Universitaria, México, DF 04510, Mexico*
[c] *CIMAV, Departamento de Química de Materiales, Chihuahua, Chihuahua, Mexico*

Available online 3 December 2007

Abstract

Defined hexagonal cylindrical pore structure SBA-15 material was synthesized as support for hydrotreating catalysts. The stability of the mesoporous material under acid and basic environments commonly used to prepare hydrotreating catalysts was investigated. The effects of the acid and basic treatments on the stability of SBA-15 and NiMo/SBA-15 catalysts were evidenced by different characterization techniques such as N_2 adsorption–desorption, X-ray diffraction (XRD), Raman Spectroscopy and high resolution transmission electron microscopy (HRTEM). Supported NiMo/SBA-15 catalysts prepared by pore volume co-impregnation in acidic, neutral and basic solutions of the Ni and Mo precursor salts were characterized to evaluate the textural and structural changes caused by the method of preparation. Characterization of the support after accelerated stability tests indicates large deterioration of the SBA-15 structural order at basic pH. The characterization results of oxide and sulfided catalysts indicate, for the catalysts prepared at high pH, an increasing presence of β–$NiMoO_4$ phase in the oxide catalysts, and a relatively lower population of MoS_2 in the sulfided catalysts. The activity of the different catalysts evaluated in the thiophene hydrodesulfurization reaction was higher for the catalysts prepared at low pH.
© 2007 Elsevier B.V. All rights reserved.

Keywords: Mesoporous silica material; SBA-15; Stability of SBA-15; Hydrodesulfurization; HRTEM; MoS_2

1. Introduction

The legislative requirements for ultra low sulfur transport fuels have resulted in new challenges in the hydrodesulfurization (HDS) processes of the refining industry. In addition to the issues related to the legislative drive for removing sulfur, refiners are also faced with a growing demand for diesel fuels. One direction of the current research for developing high-performance HDS catalysts focuses on the use of new types of supports different from alumina, which is the conventionally used support [1]. The reports in the literature indicate that HDS catalysts supported on silica display lower active phase-support interaction leading to well sulfided catalysts with higher population of the highly active type II CoMoS or NiMoS HDS catalytic sites [2]. The recent discovery of SBA-15 has opened new possibilities for the preparation of better catalysts supported on silica-based materials. SBA-15 presents several advantages such as high surface area (≈800 $m^2\ g^{-1}$) and a hexagonal arrangement of mesopores with sizes from 4 to 30 nm. Pore wall thicknesses of around 3–6 nm give SBA-15 higher thermal and hydrothermal stability than that displayed by MCM-41 [3–6]. In recent years different research groups have reported SBA-15 as promising support for hydrotreating catalysts [7–15], but less attention has been paid to the effect of preparation conditions on the stability of the catalyst support. During the preparation of the catalyst, the support might be subjected to different environments, which can deteriorate to different degrees the textural and structural properties of SBA-15. In particular, in the case of NiMo HDS catalysts, the impregnation of the Ni and Mo precursor salts on the support can be performed using either highly acidic or basic solutions. Usually, ammonium heptamolybdate and nickel nitrate, used as precursor salts, are dissolved in solution of NH_4OH (pH = 9–12), or hydrochloric acid (pH = 1–2). In the

* Corresponding author at: Departamento de Ingeniería Química, Facultad de Química, UNAM, Cd. Universitaria, México, DF 04510, Mexico.
E-mail address: jrs@servidor.unam.mx (J. Ramírez).

0920-5861/$ – see front matter © 2007 Elsevier B.V. All rights reserved.
doi:10.1016/j.cattod.2007.10.111

case of hydrotreating catalysts it is desirable to attain good dispersion and, to preserve the textural and structural integrity of the support, a low interaction of the metal precursors with the support [16]. The interaction of active phases and support will be strongly affected by the iso-electric point (IEP) of the support that in our case is around 2.5 [17], and the chemistry in solution of the precursor salts used for impregnation. It is not clear to what extent these aggressive environments used during the catalyst preparation will affect the surface area, pore volume and long range order of the SBA-15 hexagonal pore system. It is also not clear the extent of the negative consequences that these changes will have on the performance of the final catalysts.

The aim of this work is to assess the magnitude of these changes when SBA-15 is treated with acidic, neutral and basic solutions and when NiMo/SBA-15 hydrotreating catalysts are prepared by impregnation with acid, neutral and basic solutions containing the catalyst metal precursors (Ni and Mo). To this end, samples of SBA-15 were analyzed by nitrogen physisorption, X-ray diffraction and high resolution transmission electron microscopy (HRTEM) after being subjected to acidic, neutral and basic conditions during several hours. Besides, the same characterization techniques were used to evaluate the textural and structural changes of NiMo/SBA-15 catalysts prepared by pore volume impregnation using acidic, neutral and basic solutions of the Ni and Mo precursor salts (nickel nitrate and ammonium heptamolybdate, respectively). The activity of the different catalysts was evaluated in the thiophene hydrodesulfurization reaction.

2. Experimental

2.1. Synthesis of support

The SBA-15, mesoporous silica was prepared according to the procedure of Zhao et al. [3,4], using Pluronic P123 (EO_{20}-PO_{70}-EO_{20}) EO = poly-ethylene oxide) and PO = poly (propylene oxide) as templating agent. Eight grams of pluronic P123 triblock copolymer was dissolved in 160 g of 2N HCl solution, then 18.8 mL of TEOS (tetraethyl orthosilicate) and 40 mL of deionized water were added under stirring at a temperature of 40 °C for 20 h and then heated to 100 °C in a teflon bottle for 48 h. The solid product was filtered, washed with deionized water, and dried for 24 h in a desiccator. To remove the organic template; the sample was calcined at 500 °C for 6 h using a heating rate of 0.5 °C/min.

2.2. Support stability test

Accelerated stability tests were carried out with the pure support. For the acid treatments with HCl, 3.0 g of SBA-15 and 50 mL of 35% aqueous solution of hydrochloric acid (pH < 1), were stirred 12 h under reflux. For the basic treatment with NH_4OH, 3.0 g of SBA-15 with 50 mL of 28% ammonium hydroxide solution (pH ≈ 9.0) were stirred and refluxed overnight. In both cases the resulting product was recovered by filtration, washed with deionized water, dried 12 h at ambient temperature and dried in an oven at 100 °C for 4 h, then samples were calcined at 500 °C for 4 h using a heating rate 2 °C/min. Hereafter the treated supports are designated as SBA-15HCl and SBA-15Am, respectively.

2.3. Preparation of catalyst

NiMo/SBA-15 catalysts were prepared by the incipient wetness co-impregnation. Appropriate amounts of ammonium heptamolybdate and nickel nitrate to obtain catalysts with 10 wt.% Mo and 2.6 wt.% Ni were dissolved in water, HCl, or NH_4OH solutions as used for the tests with the pure support. The support was impregnated by the pore volume method with the solution containing the metal precursor salts and was left aging 12 h before drying and calcination. The nickel promoted catalysts were dried 12 h in air at 120 °C and calcined at 450 °C for 4 h.

2.4. Characterization of supports and NiMo supported catalysts

Supports and NiMo supported catalysts were characterized by nitrogen physisorption in a Quantochrome Nova 4000 equipment at liquid nitrogen temperature (−196 °C). Prior to the adsorption, the samples were outgassed for 3 h at 300 °C.

XRD patterns were recorded on a Siemens D500 diffractometer from 0 to 12 as well as 5 to 10, 2θ with a scan rate of 0.5°/min using Cu Kα radiation.

The Raman spectra were performed on a Jobin Yvon Horiba T64000 spectrometer combined with an Olympus, BX41microscope, with an argon ion laser operating at 514.5 nm at a power level of 5 mW. The spectrometer is equipped with a CCD camera detector.

HRTEM observations of sulfided catalysts were performed with a Tecnai G^2 F30 S-Twin transmission electron microscope operating a 300 kV. The microscope is equipped with a Schottky-type field emission gun and an S-Twin objective lens (Cs = 1.2 mm; Cc 1.4 mm; point to point resolution, 0.20 nm). Samples were milled in an agate mortar and ultra sonically suspended in *n*-heptane. A drop of the supernatant liquid was placed on a 3 mm diameter lacey copper grid coated with a sputtered carbon polymer. For the estimation of average length and stacking of MoS_2 more than 200 crystallites were measured.

The thiophene HDS reaction was carried out in a fixed-bed reactor operating at atmospheric pressure and 400 °C with a flow of H_2/C_4H_4S mixture of 100 mL/min. A saturator temperature of 5 °C in order to have 4.7 mol% thiophene in hydrogen. Prior to the reaction the catalyst was sulfided at 400 °C for 3 h in a flow of a CS_2/H_2 mixture. First-order rates were calculated according to the equation $x = r\,(W/F)$, where r is the rate in mol h^{-1} $g_{cat.}{}^{-1}$, x is the fractional conversion, W is the weight of the catalyst in g, and F is the flow rate of the reactant in mol h^{-1}. The particle sizes of these catalysts were 20–40 mesh and the conversions were kept below 15% to avoid diffusional limitations. Product analysis was performed by online gas chromatography.

3. Results and discussion

3.1. Characterization SBA-15

The changes in the textural properties of the SBA-15 support subjected to accelerated stability tests under basic and acid environments followed by nitrogen physisorption are presented in Figs. 1 and 2 and Table 1. N_2 adsorption–desorption isotherm pattern of SBA-15 correspond according to IUPAC to a typical irreversible type IV isotherm with H1 hysteresis. SBA-15 isotherm shows a hysteresis loop at $P/P^\circ = 0.6$–0.8, characteristic of capillary condensation inside uniform cylindrical pores. The P/P° position of the inflection points is related to the diameter in the mesoporous range and the sharpness of the step indicates uniformity in the pore size distribution.

As the pH of the surrounding media goes from acid to basic conditions the hysteresis is modified and extends to lower and higher P/P° values due to the presence of smaller and larger pores. The shape of the step at basic pH (SBA-15Am) indicates the presence of pores with different diameters and therefore not cylindrical in shape. It appears then that the structural integrity of the SBA-15 support is only maintained when the surrounding medium is highly acidic, as in the case of SBA-15HCl and that under basic pH there is significant destruction of the pore system.

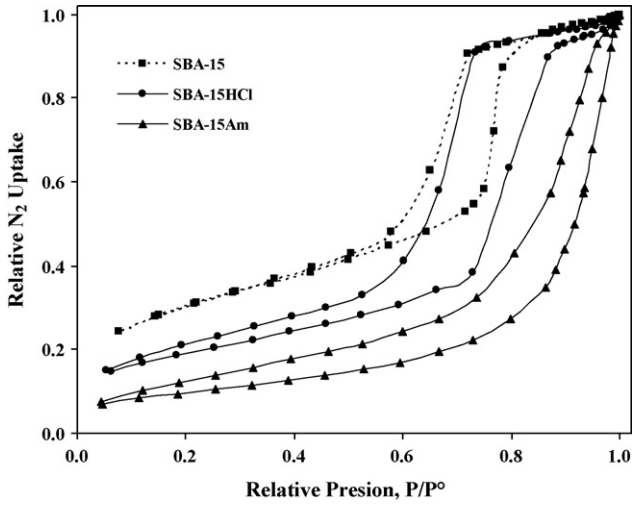

Fig. 1. Effect of treatment on textural properties of SBA-15.

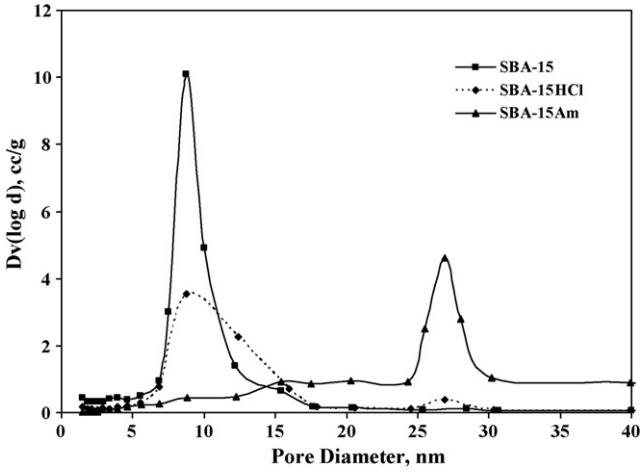

Fig. 2. Variation of pore diameter as a function of treatment.

Table 1
Textural properties of SBA-15 treated under different environments and its variation with effect of acid-base treatment

Textural properties of support						
Sample	SSA ($m^2\ g^{-1}$)	PV ($cc\ g^{-1}$)	PDmax (nm)	PVD (vol.%)		
				<5 nm	5–25 nm	>25 nm
SBA-15	779	1.2	8.7	20.6	77.0	2.3
SBA-HCl	495	1.1	8.8	8.7	86.9	4.4
SBA-Am	200	0.9	26.9	5.5	46.7	47.9

SSA: specific surface area, PV: pore volume, APD: average pore diameter, PVD: pore volume distribution.

The results of surface area and pore size distribution corroborate the deterioration of the textural structure of SBA-15 when placed in a basic media. From the as synthesized sample (SBA-15) with 779 $m^2\ g^{-1}$ surface area drops to 495 and 200 $m^2\ g^{-1}$ in the SBA-15HCl and SBA-15Am samples. The pore volume also drops and reaches a value of 0.8 for SBA-15Am compared to 1.1 cc g^{-1} for SBA-15HCl. The accelerated stability tests show then that at basic pH the texture and structure of SBA-15 is substantially altered.

The stability of the SBA-15 support material was also monitored by X-ray diffraction (XRD), the results are shown in Fig. 3. The X-ray diffraction pattern of the SBA15 support shows the three characteristic (d_{100}), (d_{110}) and (d_{200}) reflections associated with the p6mm symmetry of the hexagonal ordered pore structure. The structural integrity of the SBA-15 support is preserved under acid conditions (SBA-15HCl) but is almost completely destroyed at basic pH (SBA-15Am). For the later sample the (d_{110}) and (d_{200}) reflections characteristic of the hexagonal pore arrangement are not observed indicating the almost total destruction of the long range pore structural order in this sample.

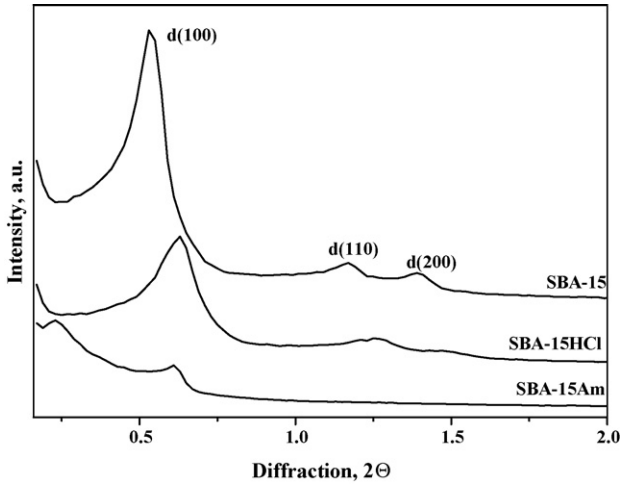

Fig. 3. X-ray diffraction of SBA-15 supports treated under different environment.

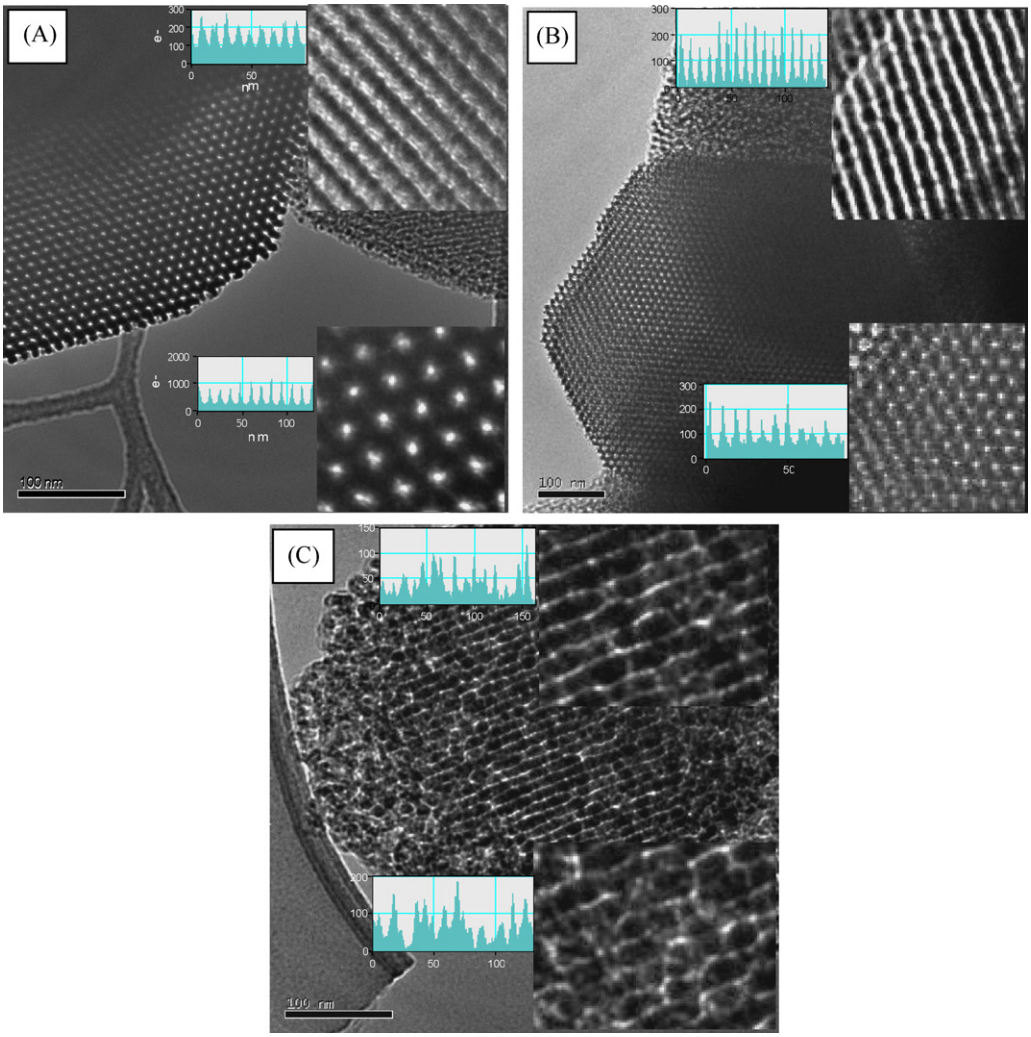

Fig. 4. HRTEM micrographs of: (A) SBA-15; (B) SBA-15HCl; (C) SBA-15Am.

To further confirm the stability of the SBA-15, samples were screened with HRTEM and the images are reported in Fig. 4A–C. As shown in the figure the freshly prepared meso-pore material is formed by well-ordered hexagonal array having typical 7–8 nm diameter of inner pores and 3–4 nm of pore wall. The inserts show the uniformity of the tube bundle array of pores, which deteriorates as the pH changes from acid to basic. The sample treated with NH_4OH presents in fact a worm-eaten appearance with pore mouths of different sizes resulting from the dissolution of some of the pore walls. Similar, results were reported by Tatsumi et al. [18] for MCM-41 and MCM-48 while others reported pore destruction at enhanced (i.e. pH $>$ 7) due to the organic swelling of template agents [19,20]. It seems clear that the preparation conditions of SBA-15 supported catalysts can alter the structural properties of the SBA-15 support.

3.2. Characterization NiMo supported catalysts

3.2.1. Oxide catalyst

To analyze if under the normal impregnating procedures of NiMo/SBA-15 catalysts the pH of the impregnating medium can alter the integrity of the SBA-15 support NiMo/SBA-15 catalysts prepared using HCl, NH_4OH and aqueous solutions were characterized and evaluated in the HDS of thiophene.

The textural properties of the NiMo/SBA-15 catalysts are presented in Fig. 5 and Table 2. The form of the isotherms suggests that at neutral and acidic conditions the structural integrity of SBA-15 remains even after nickel and molybdenum incorporation. The starting point of the hysteresis is slightly shifted to lower P/P° values when nickel and molybdenum are incorporated, indicating narrowing of the pores due to deposition of Ni and Mo on the SBA-15 pore walls.

The specific surface areas measured after NiMo loading at different pH are useful to extract information about the stability of support. The results from the textural characterization of the SBA-15 support and NiMoSBA catalysts are presented in Table 2 and Fig. 5. These results are in good agreement with those obtained in the accelerated stability tests with the supports. The textural properties of the catalysts are also considerably altered when the pH of the impregnating solution changes from acid to basic. For the NiMoSBA-NH_3 catalyst surface area drops from 779 $m^2\ g^{-1}$ exhibited by the support to 130 $m^2\ g^{-1}$. This drop in surface area suggests an almost total

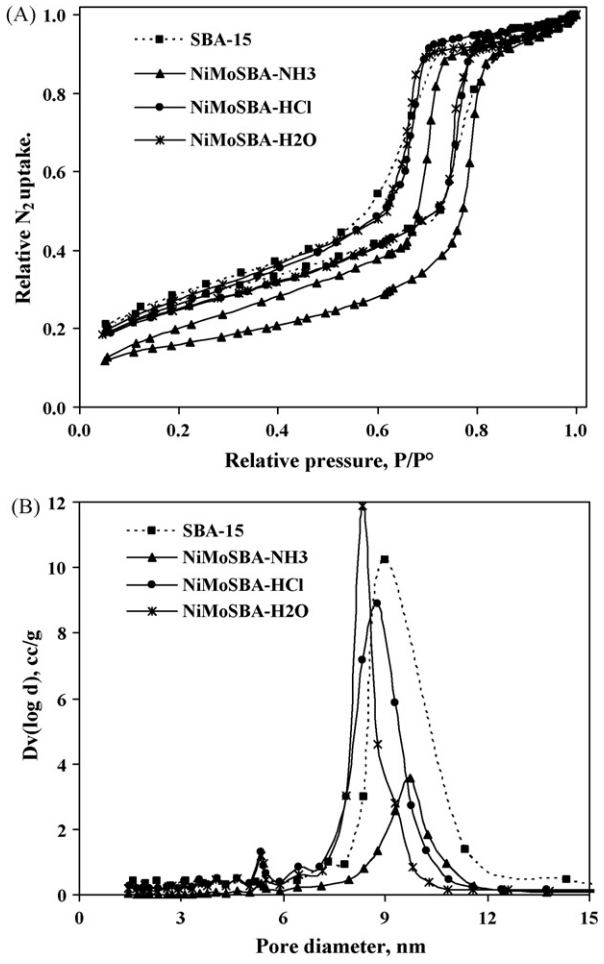

Fig. 5. (A) Effect of impregnation pH on the N_2 physisorption isotherms of NiMo catalysts. (B) Effect of impregnation pH on the pore diameter distribution of the catalysts.

destruction of the ordered porous arrangement of the SBA-15 support. In contrast, for the NiMoSBA-HCl and NiMoSBA-H_2O catalysts, prepared under acidic or mildly acidic conditions, the drops in surface area due to the impregnation of the metallic phases on the pore walls and the acidic medium used during catalyst preparation (pH = 1.0 and 4.6, respectively) were only moderate, leading to surface areas of 595 and 504 $m^2\ g^{-1}$, respectively. The destruction of the SBA support

Table 2
Textural properties of NiMo supported SBA-15 catalysts prepared with solutions of different pH

Textural properties of supported catalyst						
Sample	SSA ($m^2\ g^{-1}$)	PV ($cc\ g^{-1}$)	APD (nm)	PVD (vol.%)		
				Micro <2 nm	Meso 2–25 nm	Macro >25 nm
SBA-15	779	1.2	9.0	20.6	77.0	2.3
NiMoSBA-HCl	595	1.0	8.8	4.0	94.3	1.6
NiMoSBA-H_2O	504	0.9	8.8	4.5	93.6	1.8
NiMoSBA-NH_3	130	0.3	9.7	6.9	90.8	2.2

SSA: specific surface area, PV: pore volume, APD: average pore diameter, PVD: pore volume distribution.

pore system in the NiMoSBA-NH_3 catalyst is also evidenced by the value of the catalyst pore volume, 0.35 cc g^{-1}, compared to 1.17 cc g^{-1} of the support. In contrast, the pore volume of the catalysts prepared under acidic conditions dropped only to 1.04 and 0.88 for the NiMoSBAHCl and NiMoSBAH_2O catalysts, respectively. The pore size distribution plots of the catalysts (Fig. 5B) show that the mean pore diameter increases in the order: NiMoSBA-H_2O < NiMoSBA-HCl < NiMoSBA-NH_3. However, the mean pore size of the catalysts prepared under acidic conditions is about 7.0 nm whereas for NiMoSBA-NH_3 is near 10 nm. This latter value indicates pore dissolution of the support pore walls for the NiMoSBA-NH_3 catalyst. In contrast, the slight decrease in the mean pore diameter for NiMoSBA-HCl and NiMoSBA-H_2O can be explained as resulting from the impregnation of the metallic Ni and Mo phases on the pore walls.

The small angle X-ray diffraction patterns of the catalysts (Fig. 6A), show several changes that seem to be in agreement with the observed changes in the textural properties of the catalysts. The X-ray diffraction pattern of the SBA-15 support shows the three characteristic (d_{100}), (d_{110}) and (d_{200}) reflections associated with the p6mm symmetry of the hexagonal ordered pore structure. The diffraction patterns of

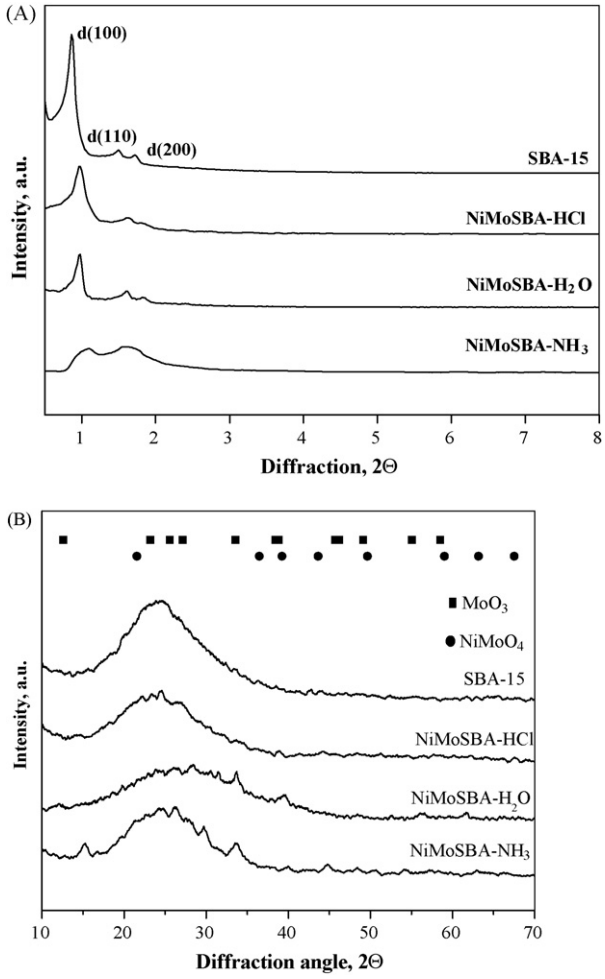

Fig. 6. (A) Low angle XRD of NiMo/SBA-15 catalyst prepared with impregnating solutions of different pH. (B) 2Θ (10–70) XRD of NiMo catalysts prepared with impregnating solutions of different pH.

the NiMoSBA-HCl and NiMoSBA-H_2O catalysts show the same peaks indicating that the integrity of the pore structure was preserved after the preparation of the catalysts. In contrast, the main diffraction peak (d_{100}) is poorly resolved for the NiMoSBA-NH_3 catalyst and the reflections (d_{110}) and (d_{200}) have completely disappeared indicating the almost total destruction of the long range pore structural order in this sample. On the other hand, the X-ray diffraction patterns for NiMo SBA-HCl, in the region (10–70, 2θ) where MoO_3 and NiO peaks appear in Fig. 6B, show no reflections other than those assigned to silica at the different impregnation pH's. This suggests that in the NiMoSBA-HCl sample the active metals are either well dispersed or present a crystal size of less than 4 nm. However, for NiMoSBA-H_2O and NiMoSBA-NH_3 some peaks which could be assigned to the presence $NiMoO_4$ are evidenced.To determine the nature of the oxide phases present on the support surface Raman analysis was used. The Raman spectra of the oxide catalysts show for NiMoSBA-H_2O and NiMoSBA-NH_3 vibrations at 957, 908 and 701 cm^{-1} corresponding to the presence of the β-$NiMoO_4$ phase [21]. These bands do not appear for NiMoSBA-HCl. The formation of different Ni and Mo phases on the support surface can be related to the interactions of the species in solution with the support. These interactions are affected mainly by the pH of the solution and the isoelectric point (IEP) of the SBA-15 support (∼2.0) [21–23]. At low pH (below the IEP), the surface of the SBA-15 support will be charged positively and the interaction of the surface with the molybdate ions in solution will be favored. In contrast at high pH (above the IEP of SBA-15), the surface of the support will be charged negatively and the molybdate ions in solution will interact more favorably with the positively charged Ni ions. This will favor the formation of Ni-Mo phases when the catalyst is calcined, and explains the presence of the β-$NiMoO_4$ phase in the calcined NiMoSBA-NH_3 and NiMoSBA-H_2O catalysts (see Fig. 7A and B). It must be considered that the species of Ni and Mo will change with the pH and the concentration in the solution. In the ammonium hydroxide solution the Ni ions will be present as $Ni(NH_3)_6^{2+}$, whereas in the HCl solution the Ni^{2+} ion will probably be present as a chloride complex, perhaps $NiCl_4^{2-}$. Likewise, the pH and concentration will affect the degree of polymerization and nature of the molybdate species present in solution. Clearly, the nature of the Ni and Mo species formed in solution will dictate their interaction with the support and will affect the nature of the phases formed during the calcination of the catalyst.

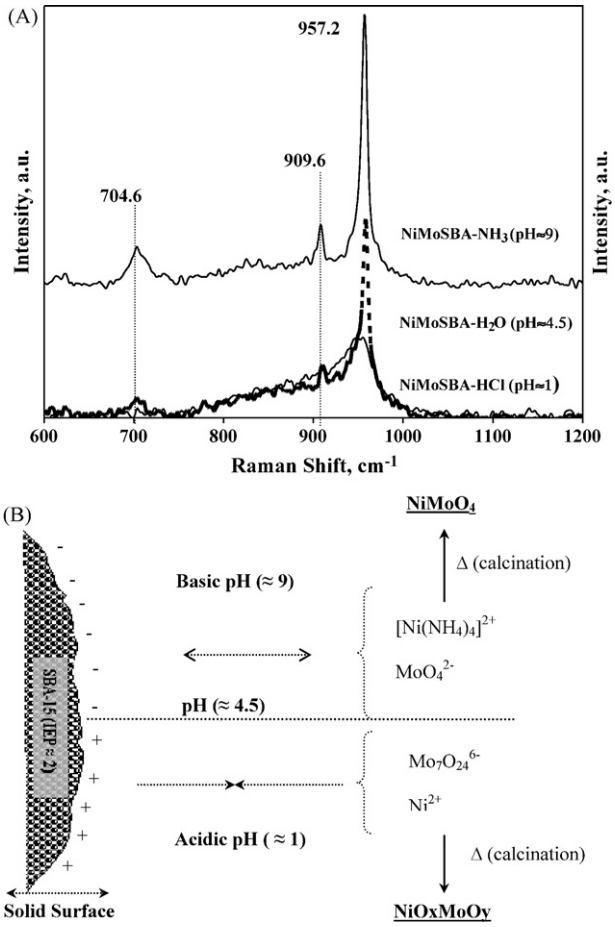

Fig. 7. (A) Raman spectra of NiMo oxide catalysts. (B) Proposed interactions of the SBA-15 surface with the Mo and Ni species in solution with variation in the pH of the impregnation medium and the phases obtained after calcination.

3.2.2. Sulfided catalysts

The presence of different phases on the support surface is expected to affect the sulfidation and dispersion of Mo and Ni phases. To enquire about this issue, HRTEM micrographs of the sulfided catalysts were taken. Electron microscopy micrographs of the different catalysts are presented in Fig. 8A–C.

All catalysts present the typical fringes of MoS_2 crystallites with different degree of stacking and sulfidation. NiMoSBA-HCl and NiMoSBA-H_2O display well sulfided MoS_2 crystallites with higher degree of stacking than NiMoSBA-NH_3. In fact the population of MoS_2 crystallites is smaller in NiMoSBA-NH_3 and the crystallites seem to be less sulfided. The possible difference in the sulfidation degree could be related to the difficulty in the sulfidation of the β-$NiMoO_4$ phase present in significant amounts in NiMoSBA-NH_3.

The average length and number of layers for the MoS_2 crystallites for the different catalysts is presented in Table 3. The length and average stacking of MoS_2 crystallites for NiMoSBA-HCl and NiMoSBA-H_2O is similar although the ratio L_{av}/N_{av}, which gives an indication of the dispersion, is higher for the former. The catalyst prepared at basic conditions, NiMoSBA-NH_3, displays shorter and less stacked MoS_2 crystallites. However, it is not possible to draw definite conclusions from the numbers in Table 3 since it appears from the same micrographs that the degree of sulfidation of all the catalysts is not the same and that NiMoSBA-NH_3 is less sulfided.

Since some of the sizes of the MoS_2 crystallites were large compared to the pore diameter of SBA-15, HRTEM micrographs of the same sample area at different tilt angles (−6°, 0°, and +10°) were made. By tilting it is possible that some MoS_2 crystallites located at the interior of the cylindrical pores that are not visible at a given electron beam angle, they will become visible after tilting the electron beam with respect to the sample.

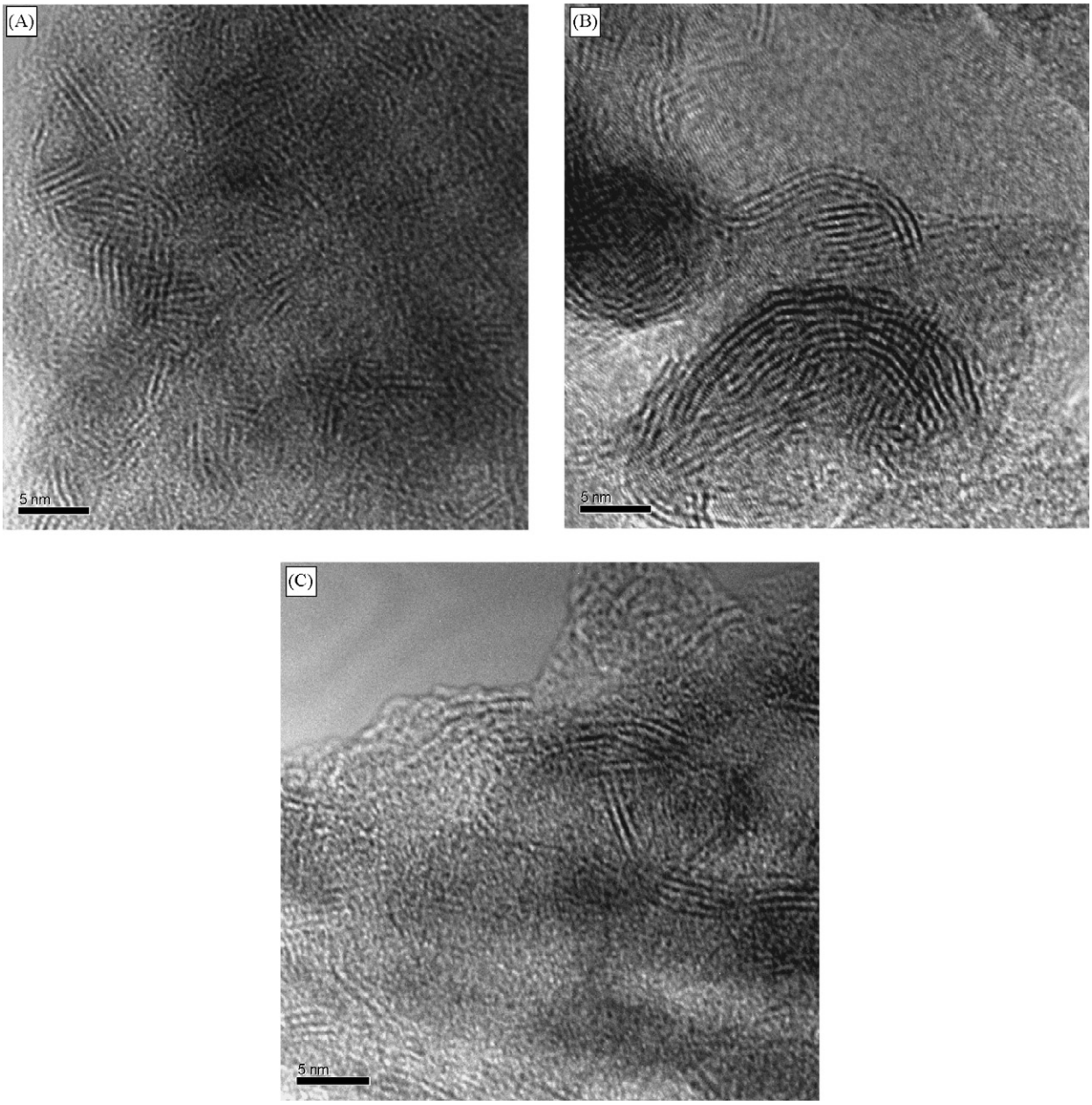

Fig. 8. HRTEM micrographs of NiMo supported catalysts over SBA-15: (A) NiMoSBA-HCl; (B) NiMoSBA-H_2O; (C) NiMoSBA-NH_3.

Fig. 9A–C, which contain micrographs taken at -6°, 0°, and 10°, respectively, show that as a result of the tilting, some MoS_2 slabs disappear while others appear. This suggests that at least part of the MoS_2 crystallites is inside the pores. Similar conclusions were reported for WS_2 over the SBA-15 support, using tilt angles of -10°, 0°, and $+10^\circ$ [13].

Table 3
Average length (L_{av}) and stacking (N_{av}) of MoS_2 crystallites (nm)

Catalyst	L_{av}	N_{av}	L_{av}/N_{av}
NiMo/SBA-HCl	3.8	3.2	1.2
NiMo/SBA-H_2O[a]	9.8	5.5	1.8
NiMo/SBA-NH_3	6.5	2.5	2.6

[a] Due to the nature of curve slabs the error may increase.

4. Catalytic activity

The steady state (after 4 h of reaction time) thiophene HDS results given in Table 4 indicate that important benefits to catalytic activity are obtained when the catalysts are impregnated under acidic medium such as for NiMoSBA-HCl (pH $\approx$ 1) and NiMoSBA-H_2O (pH de 4.5). In contrast, the HDS activity of the NiMoSBA-NH_3 catalyst, prepared at basic conditions, is three times less than that of the NiMoSBA-HCl catalyst. The reasons for the sharp decrease in HDS performance could be the solubility of the SBA-15 support material under basic conditions, which leads during catalyst preparation to the dissolution and re-precipitation of amorphous silica, decreasing the accessibility of the reactants to the Mo and Ni sulfided phases. Moreover, amorphous SiO_2

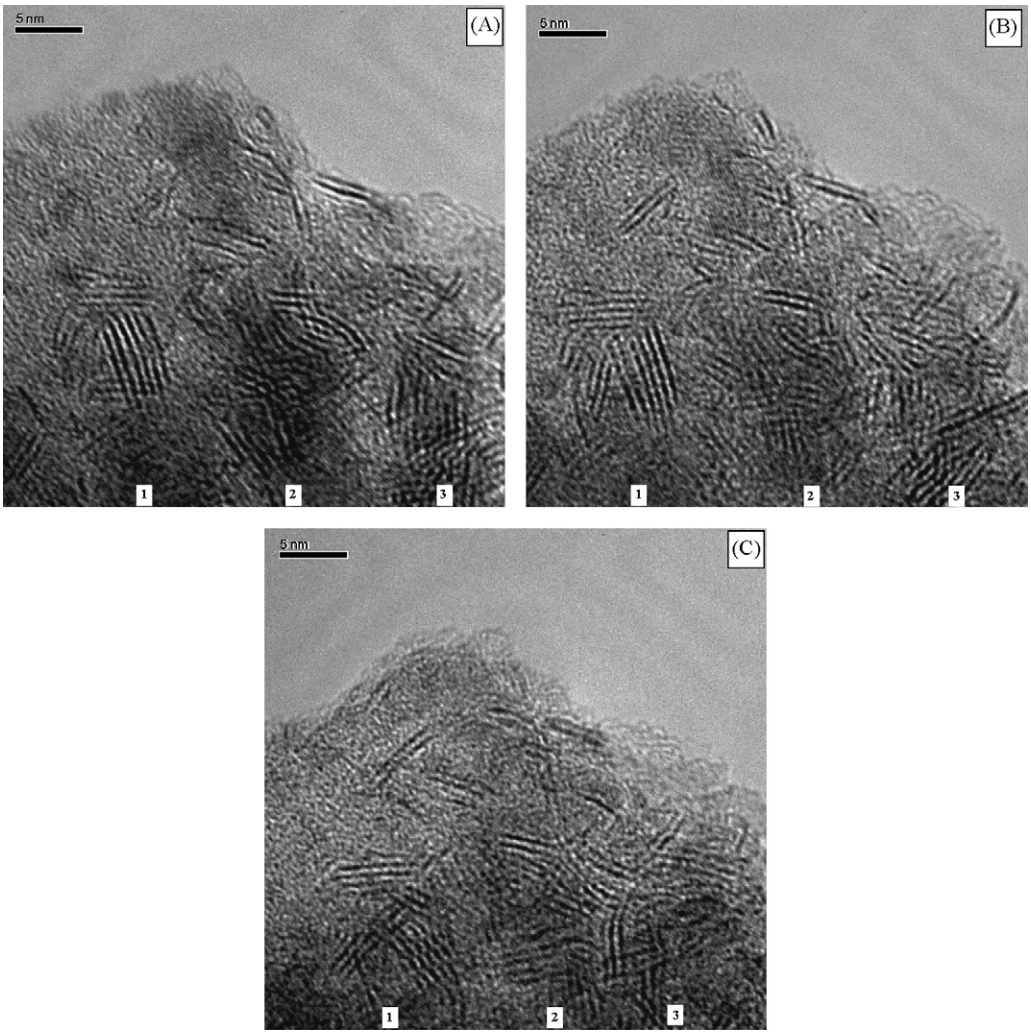

Fig. 9. Effect of rotation [(A) −6°; (B) 0°; (C) +10°] on the HRTEM of sulfided NiMo/SBA-HCl catalysts.

can re-precipitate over the active phases hindering their sulfidation. Less sulfided Mo was suggested by the characterization of the sample prepared at basic conditions. The drop in activity with pH can also be related to the presence in the oxide precursor catalysts of significant amounts of β-$NiMoO_4$, which is less prone to be sulfided or can form poorly dispersed sulfided phases [24]. As explained before, it is likely that the formation of β-$NiMoO_4$ is favored by the chemistry in solution of the Mo species and the mainly negative surface charge on the SBA-15 support (IEP = 2.0), as outlined in Fig. 7A and B.

Table 4
Thiophene HDS activity for SBA-15-supported NiMo catalysts prepared at different pH.

Catalysts	r_{HDS} (mol h^{-1} $g_{cat.}{}^{-1}$) × 10^3
NiMo/SBA-HCl	11.0
NiMo/SBA-H_2O	10.6
NiMo/SBA-NH_3	3.3

5. Conclusion

Well-defined hexagonal cylindrical pore structure of SBA-15 material was synthesized as support for hydrotreating catalysts. However, significant changes in the structure and texture of SBA-15 are induced during catalyst preparation due to the pH of the solutions used to impregnate the active phase precursors, in our case Ni and Mo. Impregnation under basic conditions using NH_4OH solutions leads to destruction of the hexagonal pore order and to significant dissolution of the pore walls, causing important drops in surface area and pore volume.

The pH of the impregnating solution can also influence the nature of the oxide Ni and Mo species present on the oxide catalyst surface. $NiMoO_4$ is present in significant amounts for catalysts prepared at basic pH with NH_4OH solutions and to a lesser extent for the catalyst prepared dissolving the salt precursors in an aqueous solution (pH = 4.5). The changes induced by the pH of the impregnating medium affect the final state of the sulfided active NiMoS phases leading to important differences in hydrodesulfurization activity of catalysts prepared under basic and acidic conditions.

For catalysts prepared in acidic conditions the structural integrity of SBA-15 is preserved, formation of $NiMoO_4$ is absent, and high catalytic activity is obtained.

Acknowledgements

One of us P. Rayo thanks CONACyT for Ph.D. fellowship. JR acknowledges financial support from CONACyT-Project 49479. We also express our appreciation to Mrs. B. Núñez-Muñoz, J.G. Espinosa and Mr. V.M. Menendez for helping in adsorption-desorption and X-ray diffraction analysis experiments.

References

[1] H. Topsøe, B. Hinnemann, J.K. Nørskov, J.V. Lauritsen, F. Besenbacher, P.L. Hansen, G. Hytoft, R.G. Egeberg, K.G. Knudsen, Catal. Today 107/108 (2005) 12–22.
[2] M.S. Rana, J. Ramirez, A. Gutiérrez-Alejandre, J. Ancheyta, L. Cedeño, S.K. Maity, J. Catal. 246 (2007) 100–108.
[3] D. Zhao, Q. Huo, J. Feng, B.F. Chmelka, G.D. Stucky, J. Am. Chem. Soc. 120 (1998) 6024–6036.
[4] D. Zhao, J. Feng, H. Qisheng, N. Melosh, G.H. Fredrickson, B.F. Chmelka, G.D. Stucky, Science 279 (1998) 548–552.
[5] H. Topsøe, B.S. Clausen, F.E. Massoth, Hydrotreating Catalysis Science and Technology, Springer-Verlag, New York, 1996.
[6] X. Cui, W.C. Zin, W.J. Cho, C.S. Ha, Mater. Lett. 59 (2005) 2257–2261.
[7] P.J. Kooyman, P. Waller, A.D. van Langeveld, C. Song, K.M. Reddy, J.A.R. van Veen, Catal. Lett. 90 (2003) 131–135.
[8] R. Mokaya, J. Phys. Chem. B 103 (1999) 10204–10208.
[9] G.M. Kumaran, S. Garg, K. Soni, M. Kumar, L.D. Sharma, G. Murali Dhar, K.S.R. Rao, Appl. Catal. A: Gen. 305 (2006) 123–129.
[10] G. Murali Dhar, G.M. Kumaran, M. Kumar, K.S. Rawat, L.D. Sharma, B.D. Raju, K.S.R. Rao, Catal. Today 99 (2005) 309–314.
[11] A. Sampieri, S. Pronier, J. Blanchard, M. Breysse, S. Brunet, K. Fajerwerg, C. Louis, G. Pérot, Catal. Today 107/108 (2005) 537–544.
[12] J. Blanchard, M. Breysse, K. Fajerwerg, C. Louis, C.-E. Hédoire, A. Sampieri, S. Zeng, D. Li, Stud. Surf. Sci. Catal. 158 B (2005) 1517–1524.
[13] L. Vradman, M.V. Landau, M. Herskowitz, V. Ezerkys, M. Talianker, S. Nikitenko, Y. Koltypin, A. Gedanken, J. Catal. 213 (2003) 163–175.
[14] O.Y. Gutierrez, G.A. Fuentes, C. Salcedo, T. Klimova, Catal. Today 116 (2006) 485–497.
[15] J.C. Amezcua, L. Lizama, C. Salcedo, I. Puente, J.M. Dominguez, T. Klimova, Catal. Today 107/108 (2005) 578–588.
[16] E. Byambajav, Y. Ohtsuka, Appl. Catal. A: Gen. 252 (2003) 193–2004.
[17] A. Sampieri, J. Blanchard, M. Breysse, K. Fajerwerg, C. Louis, S. Brunet, G. Pérot, S. Pronier, Stud. Surf. Sci. Catal. 158 A (2005) 885–892.
[18] T. Tatsumi, K.A. Koyano, Y. Tanaka, S. Nakata, Chem. Lett. 26 (1997) 469–470.
[19] D.G. Choi, S.M. Yang, J. Colloid Interface Sci. 261 (2003) 127–132.
[20] P. Chmidt-Winkel, W.W. Lukens Jr., D. Zhao, P. Yang, B.F. Chmelka, G.D. Stucky, J. Am. Chem. Soc. 121 (1999) 254.
[21] D. Dufresne, E. Payen, J. Grimblot, J.P. Bonnele, J. Phys. Chem. 85 (1981) 2344–2351.
[22] J.A. Bergwerff, M. Jansen, B.R.G. Leliveld, T. Visser, K.P. de Jong, B.M. Weckhuysen, J. Catal. 243 (2006) 292–302.
[23] J.A. Bergwerff, T. Visser, B.R.G. Leliveld, B.D. Rossenaar, K.P. de Jong, B.M. Weckhuysen, J. Am. Chem. Soc. 126 (2004) 14548–14556.
[24] D. Li, H. Xu, G.D. Guthrie Jr., J. Catal. 189 (2000) 281–296.